

Relativistic MOND Theory from Modified Entropic Gravity

A. Rostami^{1a}, K. Rezazadeh^{2b}, and M. Rostampour^{1c}

¹*Physics and Energy Engineering Department,*

Amirkabir University of Technology (Tehran Polytechnics), P.O. Box 159163-4311, Tehran, Iran

²*School of Astronomy, Institute for Research in Fundamental*

Sciences (IPM), P.O. Box 19395-5531, Tehran, Iran

(Dated: November 11, 2025)

Abstract

We derive a relativistic extension of Modified Newtonian Dynamics (MOND) within the framework of entropic gravity by introducing temperature-dependent corrections to the equipartition law on a holographic screen. Starting from a Debye-like modification of the surface degrees of freedom and employing the Unruh relation between acceleration and temperature, we obtain modified Einstein equations in which the geometric sector acquires explicit thermal corrections. Solving these equations for a static, spherically symmetric spacetime in the weak-field, low-temperature regime yields a corrected metric that smoothly approaches Minkowski space at large radii and naturally contains a characteristic acceleration scale. In the very-low-acceleration regime, the model reproduces MOND-like deviations from Newtonian dynamics while providing a relativistic underpinning for that phenomenology. We confront the theory with rotation-curve data for NGC 3198 and perform a Bayesian parameter inference, comparing our relativistic MOND (RMOND) model with both a baryons-only Newtonian model and a dark-matter halo model. We find that RMOND and the dark-matter model both fit the data significantly better than the baryons-only Newtonian prediction, and that RMOND provides particularly improved agreement at $r \gtrsim 20$ kpc. These results suggest that temperature-corrected entropic gravity provides a viable relativistic framework for MOND phenomenology, motivating further observational tests, including gravitational lensing and extended galaxy samples.

^a abasat.rostami@aut.ac.ir

^b kazem.rezazadeh@ipm.ir

^c rostampourmostafa@gmail.com

I. INTRODUCTION

The persistent mismatch between Newtonian gravity and astrophysical observations, most notably the inability of Newtonian dynamics to reproduce galactic rotation curves, has long motivated the search for alternative explanations. Among these, the dark matter (DM) hypothesis postulates the existence of a non-luminous component that reconciles theory with observation. In contrast, the Modified Newtonian Dynamics (MOND) paradigm, proposed by Milgrom [1–3], postulates that Newtonian dynamics must be modified at accelerations below a certain threshold value. Although MOND successfully accounts for galactic rotation curves and related empirical relations, it faces serious challenges in explaining gravitational dynamics on larger scales, such as those of galaxy clusters and the cosmic microwave background (CMB) [4–7].

Over the past few decades, a growing body of research has uncovered profound links between thermodynamics and gravity, reshaping our understanding of spacetime at a fundamental level. The pioneering works of Bekenstein and Hawking demonstrated that black holes behave as thermodynamic systems: they possess entropy and emit thermal radiation [8–11]. These achievements indicate that gravitational systems inherently carry thermodynamic properties, suggesting that gravity may have a statistical origin.

Another cornerstone of thermodynamic gravity is the Unruh effect [12], which associates temperature with acceleration. This effect implies that an observer undergoing constant acceleration in the quantum vacuum perceives a thermal bath at a temperature which is proportional to the observer’s acceleration [12]. This remarkable relation unites acceleration, quantum theory, and thermodynamics, and it plays a central role in modern attempts to view gravity as an emergent phenomenon. It also provides a natural context for modifying gravity through background temperature effects.

A major conceptual advance came with Jacobson’s observation [13] that the Einstein field equations themselves can be interpreted as equations of state describing a thermodynamic system. This insight paved the way for Verlinde’s entropic gravity framework [14], in which the gravitational interaction emerges as an entropic force arising from changes in information associated with the positions of material bodies. By invoking the holographic principle and the equipartition of energy on a holographic screen, Verlinde succeeded in reproducing both Newtonian gravity and Einstein’s general relativity from purely thermodynamic

considerations [14].

The holographic principle, originally proposed by 't Hooft and Susskind [15–17], states that all physical information contained within a spatial region can be fully represented by degrees of freedom residing on its boundary surface. This revolutionary concept implies that the three-dimensional universe can be viewed as a holographic projection of data encoded on a two-dimensional surface, profoundly changing our understanding of space, time, and information.

In Verlinde's approach [14], the total energy transferred to the holographic screen is assumed to be equally distributed among its microscopic degrees of freedom. In the present work, we adopt this viewpoint but allow for temperature-dependent corrections. Studies of the statistical mechanics of condensed matter have revealed that it is necessary to consider corrections to the equipartition law of energy to justify their heat capacity based on the statistical behavior of bosons at low temperatures [18, 19]. In particular, the temperature-dependent corrections to the equipartition law exhibit significant effects at low temperatures.

Moreover, in Verlinde's emergent gravity framework [20], the presence of positive dark energy gives rise to a thermal *volume law* contribution to the entropy, which becomes dominant precisely at the cosmological horizon. This contribution competes with the usual *area law* entanglement entropy, and the interplay between the two leads to nontrivial gravitational phenomena at sub-Hubble scales. In particular, due to this competition, the microscopic de Sitter states fail to thermalize below the Hubble scale and instead exhibit memory effects, manifesting as an entropy displacement induced by the presence of matter. The emergent gravitational dynamics then include an additional, “dark” elastic response force associated with this entropy displacement. Verlinde shows that the magnitude of this extra force can be expressed in terms of the baryonic mass, Newton's constant, and the Hubble acceleration scale $a_0 = cH_0$, and provides evidence that this mechanism can account for the galactic and cluster-scale phenomena usually attributed to dark matter. Moreover, it is argued that both dark energy and the apparent dark matter effects originate from a common microscopic mechanism related to the emergent nature of spacetime and gravity. Empirically, the transition to this “dark” gravitational regime occurs when the gravitational acceleration drops below the critical scale, as first emphasized by Milgrom [1–3], which also corresponds to a characteristic surface mass density threshold observed in galactic dynamics.

In Hossenfelder's covariant extension of Verlinde's emergent gravity framework [21], a

generally covariant Lagrangian is constructed which allows for an improved interpretation of the underlying mechanism of emergent gravitational dynamics. In this model, de Sitter space is effectively filled with a vector field that couples directly to baryonic matter and, through a “dragging” effect, mimics an additional gravitational force akin to dark matter. The covariant equation of motion is solved in a Schwarzschild background, yielding correction terms to the non-covariant expression first proposed by Verlinde. Furthermore, in this scheme, the same vector field can also reproduce the effect of dark energy, thereby offering a unified description of dark matter and dark energy phenomena within an emergent-gravity paradigm.

The thermodynamic interpretation of gravity thus offers a promising route to overcome the limitations of MOND. In particular, introducing temperature corrections to the entropic formulation of gravity allows one to retain MOND’s empirical successes at galactic scales while embedding them in a consistent relativistic and thermodynamic framework.

The original MOND proposal was purely non-relativistic and could not account for phenomena such as gravitational lensing or cosmological evolution. In this work, we seek to construct a *relativistic extension of MOND* derived from entropic gravity with temperature-dependent corrections. Specifically, we aim to embed MOND within a modified Einstein framework in which the geometric sector of the field equations acquires thermal modifications. This approach not only provides a relativistic foundation for MOND but also establishes an explicit link between spacetime geometry and thermodynamic quantities such as entropy and temperature.

This work builds upon previous studies in both the entropic gravity and MOND literature. The foundational work of Verlinde [14], who proposed that gravity emerges from thermodynamic principles, provides a conceptual basis for our model. We extend his framework by introducing thermal corrections to the equipartition law, allowing for a more direct connection to MOND. Additionally, our work resonates with Milgrom’s original MOND proposal [1], as well as later attempts to modify gravity in a relativistic context, such as those by Bekenstein [22] and Skordis and Zlosnik [7], who explored relativistic versions of MOND. Our model also contributes to ongoing efforts to modify gravity in ways that do not require non-baryonic dark matter, echoing the ideas of Famaey and McGaugh [23] and McGaugh [24], who have worked on explaining galaxy dynamics without invoking dark matter.

By embedding MOND in the context of entropic gravity, we provide a fresh perspective on

the long-standing debate between modified gravity and dark matter. The model presented here offers a possible resolution to the mystery of dark matter by suggesting that the effects attributed to dark matter might instead be explained by modifications to gravity itself, particularly at large galactic scales.

To achieve this goal, we exploit and solve the modified Einstein equations for a static, spherically symmetric spacetime, obtaining the modified form of the metric in the regime of extremely weak gravitational fields. The resulting metric naturally dominates for the accelerations below a characteristic acceleration scale that provides a theoretical underpinning for the phenomenological constant a_0 in MOND. Finally, we confront our model with astrophysical data by comparing its predictions for galactic rotation curves with observations. In particular, we examine the galaxy NGC 3198 and compare the results of our relativistic MOND model with those from both the classical Newtonian dynamics (ND) and dark-matter (DM) frameworks.

Our study proceeds as follows. In Sec. II, we first reformulate the Debye model to describe the microscopic degrees of freedom on a two-dimensional holographic surface. Building on this foundation, in Sec. III, we derive the modified entropic gravity equations that include temperature corrections and explore their consequences for a static, spherically symmetric metric. In Sec. IV, we assess the consistency of our results with observational data, demonstrating that the proposed framework can account for galactic dynamics without invoking dark matter. Finally, in Sec. V, we summarize our results and discuss further directions of our model.

II. GENERALIZED EINSTEIN EQUATIONS

We begin with the holographic principle, which states that the number of degrees of freedom (N) on a holographic screen \mathcal{S} is proportional to its area [14],

$$N = \frac{A}{\ell_P^2}, \quad (1)$$

where A is the area of the two-dimensional boundary and $\ell_P = \sqrt{\hbar G/c^3}$ is the Planck length. Throughout the present work, the analysis is performed in natural units where $c = \hbar = k_B = 1$. In Sec. IV, where we compare the results of the theoretical model with experimental observations, it is useful to explicitly preserve the explicit form of these

constants in the mathematical equations.

We then invoke our generalized equipartition law for the energy E of these N bits,

$$E = \frac{1}{2}NTf(T). \quad (2)$$

Here, $f(T)$ is a general statistical correction function which depends on the temperature T and accounts for quantum-statistical effects. Here, it is appropriate to introduce the variable $x \equiv T_{\text{ref}}/T = a_{\text{ref}}/a$, which is typically a dimensionless ratio, and T_{ref} refers to some fundamental reference temperature (like the Debye temperature T_D in the specific model), and T is the Unruh temperature of the screen.

The only necessary physical constraint on $f(T)$ is that it must recover classical physics in the high-temperature limit,

$$\lim_{T \rightarrow \infty} f(T) = \lim_{x \rightarrow 0} f(x) = 1. \quad (3)$$

The asymptotic behavior of this function can be determined either from a theoretical standpoint, by making certain assumptions about the energy distribution function, or from a phenomenological perspective, by requiring consistency between the final result and observational data. In this paper, we adopt the latter approach and find that the best agreement with observations within this model occurs when

$$\lim_{T \rightarrow 0} f(T) = \lim_{x \rightarrow \infty} f(x) \sim \frac{C}{x^{2+\delta}}, \quad (4)$$

where δ is a constant whose value is much smaller than unity. By combining these principles and using the mass-energy equivalence $E = M$, we define the total **thermodynamic mass** M_{th} enclosed by the screen \mathcal{S} as an integral over its area,

$$M_{\text{th}} = \int dM = \int_{\mathcal{S}} \left(\frac{1}{2G\hbar} Tf(T) \right) dA. \quad (5)$$

To express this covariantly, we identify the temperature T with the Unruh temperature for a static observer following a timelike Killing vector field ξ^a . This temperature is given by

$$T = \frac{\hbar a}{2\pi}, \quad (6)$$

where the acceleration $a = e^\phi N^b \nabla_b \phi$. Here, $\phi = \frac{1}{2} \ln(-\xi^a \xi_a)$ is the redshift potential and N^b is the unit normal to the equipotential screen \mathcal{S} .

Substituting this covariant temperature $T = \frac{\hbar}{2\pi} e^\phi N^b \nabla_b \phi$ gives our final expression for the thermodynamic mass [25, 26],

$$M_{\text{th}} = \int_{\mathcal{S}} \left(\frac{1}{2G\hbar} \right) \left(\frac{\hbar}{2\pi} e^\phi N^b \nabla_b \phi \right) f(T) dA. \quad (7)$$

This equation is the thermodynamic definition of the mass enclosed by the screen, modified by the general statistical function $f(T)$.

Next, we seek a purely geometric definition of mass, M_{geo} , to equate with M_{th} . In standard General Relativity, the Komar mass M_K is given by [27]

$$M_K = -\frac{1}{8\pi G} \int_{\mathcal{S}} \nabla^a \xi^b d\mathcal{S}_{ab}. \quad (8)$$

This integral is equivalent to

$$M_K = \frac{1}{4\pi G} \int_{\mathcal{S}} (e^\phi N^b \nabla_b \phi) dA. \quad (9)$$

Comparing M_K from Eq. (9) with our M_{th} in Eqs. (7), we see that

$$M_{\text{th}} = \int_S f(T) dM_K. \quad (10)$$

This result motivates our central postulate: The correct geometric mass M_{geo} in this generalized entropic gravity model is a modified Komar integral, where the scalar correction function $f(T)$ is inserted into the integrand,

$$M_{\text{geo}} \equiv -\frac{1}{8\pi G} \int_{\mathcal{S}} f(T) \nabla^a \xi^b d\mathcal{S}_{ab}. \quad (11)$$

We now use the generalized Stokes' theorem

$$\oint_S \omega = \int_{\Sigma} d\omega, \quad (12)$$

to transform this 2-surface integral (over \mathcal{S}) into a 3-volume integral (over the enclosed hypersurface Σ). For an antisymmetric tensor field B^{ab} , this theorem indicates [28]

$$\oint_S B^{ab} d\mathcal{S}_{ab} = 2 \int_{\Sigma} \nabla_b B^{ab} d\Sigma_a. \quad (13)$$

Applying this to M_{geo} in Eq. (11) with $B^{ab} = f(T) \nabla^a \xi^b$, we find

$$M_{\text{geo}} = -\frac{1}{8\pi G} \left(2 \int_{\Sigma} \nabla_b [f(T) \nabla^a \xi^b] d\Sigma_a \right). \quad (14)$$

Using the product rule for the covariant derivative,

$$M_{\text{geo}} = -\frac{1}{4\pi G} \int_{\Sigma} [(\nabla_b D(x))(\nabla^a \xi^b) + f(T)(\nabla_b \nabla^a \xi^b)] d\Sigma_a. \quad (15)$$

We simplify the second term using two identities for the Killing vector ξ^a [27],

$$\nabla_b \nabla^a \xi^b = -\nabla_b \nabla^b \xi^a, \quad (16)$$

$$\nabla_b \nabla^b \xi^a = -R_c^a \xi^c. \quad (17)$$

These imply

$$\nabla_b \nabla^a \xi^b = R_c^a \xi^c. \quad (18)$$

Substituting this into our integral (15) for the geometrical mass, we obtain

$$M_{\text{geo}} = -\frac{1}{4\pi G} \int_{\Sigma} [\nabla^a \xi^b \nabla_b f(T) + f(T) R_c^a \xi^c] d\Sigma_a. \quad (19)$$

For a spacelike hypersurface Σ , the directed surface element is $d\Sigma_a = -n_a d\Sigma$, where n^a is the future-pointing unit normal. Consequently, the above equation turns into

$$M_{\text{geo}} = \frac{1}{4\pi G} \int_{\Sigma} [f(T) R_{ac} \xi^c + \nabla_a \xi^c \nabla_c f(T)] n^a d\Sigma. \quad (20)$$

This expression represents the total mass of the spacetime purely in terms of its generalized, statistically-modified geometry.

The final step is to equate this geometric definition of mass M_{geo} with the physical definition of mass derived from the stress-energy tensor \mathcal{T}_{ab} . This matter-energy mass M_{matter} is given by [27],

$$M_{\text{matter}} = 2 \int_{\Sigma} \left(\mathcal{T}_{ab} - \frac{1}{2} \mathcal{T} g_{ab} \right) n^a \xi^b d\Sigma. \quad (21)$$

The fundamental principle of gravity, $M_{\text{geo}} = M_{\text{matter}}$, implies

$$\frac{1}{4\pi G} \int_{\Sigma} [f(T) R_{ac} + \nabla_a \xi^c \nabla_c f(T) g_{bc}] n^a \xi^c d\Sigma = 2 \int_{\Sigma} \left(\mathcal{T}_{ac} - \frac{1}{2} \mathcal{T} g_{ac} \right) n^a \xi^c d\Sigma, \quad (22)$$

where we have relabeled indices $b \rightarrow c$ for direct comparison. Since this equivalence must hold for any arbitrary integration volume Σ , any time-translation Killing field ξ^c , and any normal field n^a , the tensor-valued integrands must be equal. This yields the generalized Einstein field equations [25, 26]

$$f(T) R_{ab} - e^{-2\phi} \xi_b \nabla_a \xi^c \nabla_c f(T) = 8\pi G \left(\mathcal{T}_{ab} - \frac{1}{2} \mathcal{T} g_{ab} \right). \quad (23)$$

This is the most general form of the modified field equations, emerging from the premise that the holographic principle is subject to a non-classical statistical correction $f(T)$, which is not necessarily the Debye function. In the limit of high temperatures which are corresponding to strong gravitational fields, we have $f(T) = 1$, and the above equation reduces to the standard Einstein equations. But at low temperatures, which correspond to the regime of very weak gravitational fields, the effects of temperature corrections may cause the theory of gravity to be quite different from Einstein's general relativity.

III. SOLUTION OF MODIFIED EINSTEIN EQUATIONS

In this section, we are primarily interested in the solution of the modified Einstein equations (23) for a static, spherically symmetric space-time with the line element

$$ds^2 = -A(r)dt^2 + B(r)dr^2 + r^2(d\theta^2 + \sin^2\theta d\phi^2). \quad (24)$$

In this equation, $A(r)$ and $B(r)$ represent the metric coefficients, which are functions of the radial coordinate r . Our goal in the following is to determine the analytical form of these coefficients by solving the modified Einstein equations.

The Christoffel symbols of the second kind are given by the following equation

$$\Gamma_{\mu\nu}^\lambda = \frac{1}{2}g^{\lambda\sigma}(\partial_\mu g_{\nu\sigma} + \partial_\nu g_{\mu\sigma} - \partial_\sigma g_{\mu\nu}). \quad (25)$$

Using this, the non-zero Christoffel symbols for the metric (24) are obtained as

$$\Gamma_{tr}^t = \Gamma_{rt}^t = \frac{A'}{2A}, \quad (26)$$

$$\Gamma_{tt}^r = \frac{A'}{2B}, \quad \Gamma_{rr}^t = \frac{B'}{2B}, \quad \Gamma_{\theta\theta}^r = -\frac{r}{B}, \quad \Gamma_{\phi\phi}^r = -\frac{r\sin^2\theta}{B}, \quad (27)$$

$$\Gamma_{r\theta}^\theta = \Gamma_{\theta r}^\theta = \frac{1}{r}, \quad \Gamma_{\phi\phi}^\theta = -\sin\theta\cos\theta, \quad (28)$$

$$\Gamma_{r\phi}^\phi = \Gamma_{\phi r}^\phi = \frac{1}{r}, \quad \Gamma_{\theta\phi}^\phi = \Gamma_{\phi\theta}^\phi = \cot\theta. \quad (29)$$

Now, we can calculate the Riemann tensor, which is given by the following equation

$$R_{\sigma\mu\nu}^\rho = \partial_\mu\Gamma_{\nu\sigma}^\rho - \partial_\nu\Gamma_{\mu\sigma}^\rho + \Gamma_{\mu\lambda}^\rho\Gamma_{\nu\sigma}^\lambda - \Gamma_{\nu\lambda}^\rho\Gamma_{\mu\sigma}^\lambda. \quad (30)$$

The Ricci tensor is obtained by contracting the Riemann tensor through $R_{\mu\nu} \equiv R_{\mu\lambda\nu}^\lambda$. The

non-zero components of the Ricci tensor for the metric (24) are as follows

$$R_{tt} = \frac{A''}{2B} - \frac{A'B'}{4B^2} - \frac{A'^2}{4AB} + \frac{A'}{rB}, \quad (31)$$

$$R_{rr} = -\frac{A''}{2A} + \frac{A'B'}{4AB} + \frac{A'^2}{4A^2} + \frac{B'}{rB}, \quad (32)$$

$$R_{\theta\theta} = 1 - \frac{rA'}{2AB} + \frac{rB'}{2B^2} - \frac{1}{B}, \quad (33)$$

$$R_{\phi\phi} = \sin^2 \theta R_{\theta\theta} = \sin^2 \theta \left(1 - \frac{rA'}{2AB} + \frac{rB'}{2B^2} - \frac{1}{B} \right). \quad (34)$$

The Ricci tensor can be further contracted via $R \equiv R_\mu^\mu$ to give the Ricci scalar as

$$R = -\frac{A''}{AB} + \frac{A'B'}{2AB^2} + \frac{A'^2}{2A^2B} + \frac{2B'}{rB^2} - \frac{2A'}{rAB} + \frac{2}{r^2} - \frac{2}{r^2B}. \quad (35)$$

We are looking for the solution to the gravitational field equation in a vacuum. Therefore, the stress-energy tensor vanishes

$$\mathcal{T}_\nu^\mu = 0, \quad (36)$$

As a result, the modified Einstein equations (23) take the following form

$$f(T)R_{\mu\nu} - e^{-2\phi}\xi_\nu\nabla_\mu\xi^\lambda\partial_\lambda f(T) = 0. \quad (37)$$

With our complete characterization of the spacetime geometry and explicit Christoffel symbols at hand, we can now proceed to determine the Killing vector in our setting. For this purpose, we should find an appropriate solution to the Killing equation,

$$\nabla_\mu\xi_\nu + \nabla_\nu\xi_\mu = 0, \quad (38)$$

which provides all the required symmetries. Using the covariant derivative

$$\nabla_\mu\xi_\nu = \partial_\mu\xi_\nu - \Gamma_{\mu\nu}^\lambda\xi_\lambda, \quad (39)$$

we arrive at

$$\partial_\mu\xi_\nu + \partial_\nu\xi_\mu - 2\Gamma_{\mu\nu}^\lambda\xi_\lambda = 0, \quad (40)$$

where the covariant Killing vector is given by

$$\xi_\mu = g_{\mu\nu}\xi^\nu = (-A\xi^t, B\xi^r, r^2\xi^\theta, r^2\sin^2\theta\xi^\phi). \quad (41)$$

The metric's symmetries yield four sets for the Killing vectors:

1. Time translation: Owing to the t -independence of the metric (24), the vector $\xi^\mu = (1, 0, 0, 0)$ satisfies all Killing equations (40), confirming that it is a Killing vector.

2. Rotation around the z -axis: Because the metric is independent of ϕ , the vector $\xi^\mu = (0, 0, 0, 1)$ satisfies all the equations (40), and thus represents another Killing vector..
3. Rotation around the x -axis: Due to the spherical symmetry of the metric, the vector $\xi^\mu = (0, 0, \sin \phi, \cot \theta \cos \phi)$ also satisfies the Killing equations (40), corresponding to a rotation around the x -axis.
4. Rotation around the y -axis: Similarly, the vector $\xi^\mu = (0, 0, -\cos \phi, \cot \theta \sin \phi)$ fulfills Eq. (40), representing a rotation around the y -axis.

In this section, we were able to extract valuable insights regarding the symmetries of the problem. These symmetries not only help us understand the underlying structure of the space-time but also simplify the subsequent analysis. However, the main focus of our analytical computations will be devoted to the case of *time translation symmetry*, which plays a fundamental role in the conservation of energy.

At this stage, we have established all the necessary information required to proceed with the evaluation of the field equations. Therefore, we now focus on carrying out the explicit computations of the field equations based on the previously obtained results. Assuming the time-transition symmetry, we substitute the Killing vector $\xi^\mu = (1, 0, 0, 0)$ into Eq. (37). We also note that for the spherically symmetric static metric (24), the gravitational acceleration is only a function of the radial coordinate r and, as a result, the temperature T will be only a function of r . Hence, the function $f(T)$ will also depend only on r . With these considerations, the components of Einstein's equations (37) are obtained as follows

$$f(r) \left(\frac{A''}{2B} - \frac{A'B'}{4B^2} - \frac{A'^2}{4AB} + \frac{A'}{rB} \right) + \frac{A'f'(r)}{2B} = 0, \quad (42)$$

$$f(r) \left(-\frac{A''}{2A} + \frac{A'B'}{4AB} + \frac{A'^2}{4A^2} + \frac{B'}{rB} \right) = 0, \quad (43)$$

$$f(r) \left(1 - \frac{rA'}{2AB} + \frac{rB'}{2B^2} - \frac{1}{B} \right) = 0. \quad (44)$$

Combining Eqs. (42) and (43) to eliminate A'' , we reach the following equation

$$BA' (rf' + 2f) + 2AfB' = 0. \quad (45)$$

Also, it is obvious that Eq. (44) can be simplified to

$$1 - \frac{rA'}{2AB} + \frac{rB'}{2B^2} - \frac{1}{B} = 0. \quad (46)$$

Eqs. (45) and (46) are the two main equations in our work to determine the two coefficients $A(r)$ and $B(r)$ in the metric (24).

If the form of the function f is explicitly known in terms of r , then Eqs. (45) and (46) determine the metric coefficients as follows

$$A(r) = C_1 \exp \left[-4e^{C_2} \int \frac{f(r)}{r(rf'(r) + 4f(r)) \left[e^{C_2} + \exp \left(\int \frac{2rf'(r) + 4f(r)}{r^2f'(r) + 4rf(r)} dr \right) \right]} dr \right], \quad (47)$$

$$B(r) = \frac{1}{\exp \left[C_2 - \int \frac{2rf'(r) + 4f(r)}{r^2f'(r) + 4rf(r)} dr \right] + 1}, \quad (48)$$

where C_1 and C_2 are constant parameters. Since in our work, the explicit dependence of the function f on r is not known, therefore, the above two equations are not applicable in our approach, and we have to use the differential equations (45) and (46) directly.

In our model, the function f is a function of gravitational acceleration a . To determine gravitational acceleration, we should use the geodesic equations, which are given generally by

$$\frac{\partial^2 x^\mu}{\partial \tau^2} + \Gamma_{\nu\lambda}^\mu \frac{\partial x^\lambda}{\partial \tau} \frac{\partial x^\nu}{\partial \tau} = 0. \quad (49)$$

For the metric (24), the above equation leads to the following equations

$$\frac{\partial^2 t}{\partial \tau^2} + \frac{A'}{A} \frac{\partial t}{\partial \tau} \frac{\partial r}{\partial \tau} = 0, \quad (50)$$

$$\frac{\partial^2 r}{\partial \tau^2} + \frac{A'}{2B} \left(\frac{\partial t}{\partial \tau} \right)^2 + \frac{B'}{2B} \left(\frac{\partial r}{\partial \tau} \right)^2 - \frac{r}{B} \left(\frac{\partial \theta}{\partial \tau} \right)^2 - \frac{r \sin^2 \theta}{B} \left(\frac{\partial \phi}{\partial \tau} \right)^2 = 0, \quad (51)$$

$$\frac{\partial^2 \theta}{\partial \tau^2} - \sin \theta \cos \theta \left(\frac{\partial \phi}{\partial \tau} \right)^2 + \frac{2}{r} \left(\frac{\partial r}{\partial \tau} \right) \left(\frac{\partial \theta}{\partial \tau} \right) = 0, \quad (52)$$

$$\frac{\partial^2 \phi}{\partial \tau^2} + 2 \cot \theta \left(\frac{\partial \theta}{\partial \tau} \right) \left(\frac{\partial \phi}{\partial \tau} \right) + \frac{2}{r} \left(\frac{\partial r}{\partial \tau} \right) \left(\frac{\partial \phi}{\partial \tau} \right) = 0. \quad (53)$$

In our analysis, we deal with very weak gravitational fields and low velocities that are significantly lower than the speed of light. Taking these assumptions into account, we can ignore the second term on the left side of Eq. (50) compared to the first term [29]. Similarly, in (51), only the first two terms remain on the left side, and the other terms can be neglected in front of them [29]. Therefore, Eqs. (50) and (51) can be rewritten approximately as

$$\frac{\partial^2 t}{\partial \tau^2} \approx 0. \quad (54)$$

$$\frac{\partial^2 r}{\partial \tau^2} + \frac{A'}{2B} \left(\frac{\partial t}{\partial \tau} \right)^2 \approx 0. \quad (55)$$

Using these equations, the gravitational acceleration is obtained in our model as

$$a = \frac{\partial^2 r}{\partial t^2} \approx -\frac{A'}{2B}. \quad (56)$$

This is the general form of the gravitational acceleration for the static, spherically metric (24) in the regime of weak gravitational fields and low velocities.

Now, we use the above acceleration in the differential equations (45) and (46). In this way, we find that the following solutions satisfy the modified Einstein equations

$$A(r) = 1 + C_A r^\epsilon, \quad (57)$$

$$B(r) = \frac{(2 + \epsilon)(1 + C_A r^\epsilon)}{2(1 + C_A r^\epsilon) + \epsilon}. \quad (58)$$

Also, the temperature correction function is determined in our scenario as

$$f(r) = C_1 (2 + 2C_A r^\epsilon + \epsilon)^{\frac{2}{2+\epsilon}} r^{-\frac{4(1+\epsilon)}{2+\epsilon}}, \quad (59)$$

In these equations, C_A is the integration constant and ϵ is a constant parameter whose value is much smaller than unity. We will see later that this parameter is of the same order as the δ parameter in Eq.(4). The above two equations are the solutions of the modified Einstein equations in our relativistic MOND scenario that determine the curvature of space-time in the very weak gravitational regime. In deriving these equations, we have imposed the condition of asymptotically flatness for both the metric coefficients. Therefore, these coefficients satisfy the asymptotic behaviors $A(r) \approx 1$ and $B(r) \approx 1$ in the limit of very weak gravitational fields. Considering these conditions, Eq. (59) can be approximated as

$$f(r) \approx \tilde{C} (2 + \epsilon)^{\frac{2}{2+\epsilon}} r^{-\frac{4(1+\epsilon)}{2+\epsilon}}, \quad (60)$$

where \tilde{C} is a constant parameter. On the other hand, we assume the asymptotic form (4), we obtain this function as

$$f(r) \approx 2^{-(2+\delta)} C a_{\text{ref}}^{-\delta-2} C_A^{\delta+2} \epsilon^{\delta+2} r^{(\delta+2)(\epsilon-1)}. \quad (61)$$

By equating Eqs. (60) and (61), the parameters δ and \tilde{C} are determined as

$$\delta = \frac{2\epsilon(3 + \epsilon)}{2 - \epsilon - \epsilon^2} \approx 3\epsilon, \quad (62)$$

$$\tilde{C} = 2^{-\frac{4(1+\epsilon)}{2-\epsilon-\epsilon^2}} (2 + \epsilon)^{-\frac{2}{2+\epsilon}} C \left(\frac{C_A \epsilon}{a_{\text{ref}}} \right)^{\frac{4(1+\epsilon)}{2-\epsilon-\epsilon^2}} \approx \frac{C}{8} \left(\frac{C_A \epsilon}{a_{\text{ref}}} \right)^2. \quad (63)$$

In Eq. (62), it is clear that the parameter δ is of the order of the parameter ϵ , which is much smaller than unity.

By using Eqs. (57) and (58) in Eq. (56), the magnitude of the gravitational acceleration is obtained as

$$|a| \approx \frac{1}{2} |C_A \epsilon| r^{-1+\epsilon}. \quad (64)$$

The magnitude of the gravitational acceleration is related to the rotational velocity by $|a| = v^2/r$. Consequently, we find that the rotational velocity of a test particle in the vicinity of the holographic screen in our RMOND model is given by

$$v = \sqrt{r|a|} \approx \sqrt{\frac{|C_A \epsilon|}{2}} r^{\epsilon/2}. \quad (65)$$

In the next section, we use the above equation to estimate the rotational velocities of stars located at far distances from the center of the galaxy and compare the results of our model with the observational results.

IV. COMPARISON WITH OBSERVATIONAL DATA

Our main goal in this section is to test the consistency of our relativistic MOND model in light of the observational data. To do so, we evaluate the rotational velocity curves of the stars at the edge of a galaxy in this model and compare the results with the measured values. In our work, we use data from the galaxy NGC 3198, which belongs to the SPARC catalog and whose data are publicly available ¹. The catalog we use contains results for 43 stars in which the rotational velocities are listed as a function of distance. In this section, in order to be able to estimate the observational quantities in our model correctly and in the correct dimensions, we need to reintroduce the fundamental constants G , c , and \hbar to the theoretical equations.

We also compare our RMOND model results with those of the classical Newtonian dynamics (ND) model and the model including dark matter (DM). In the ND and DM models, the gravitational acceleration is given by the following equation

$$a = \frac{GM(r)}{r^2}. \quad (66)$$

In the ND model, the mass $M(r)$ only includes the baryonic mass of the galaxy disk $M_d(r)$, but in the DM model, this mass includes both the baryonic mass of the galaxy disk of

¹ https://astroweb.cwru.edu/SPARC/Rotmod_LTG.zip

the galaxy $M_d(r)$ and the mass of the dark matter halo $M_{DM}(r)$. The mass of the galaxy disk is the sum of the mass of the stars in that galaxy, and here we have neglected the mass of the interstellar gas. We assume an exponential profile for the surface mass density of the disk with the radial distance r as [30]

$$\sigma(r) = \sigma_0 e^{-r/R_d}. \quad (67)$$

In this equation, σ_0 is the surface mass density at the center of the galaxy and R_d is the characteristic radius of the disk at which the disk mass density declines to the value of σ_0/e . By integrating the above equation on the surface of the disk, we obtain the mass of the galaxy disk as

$$M_d(r) = \int_0^r (2\pi r') \sigma(r') dr' = 2\pi R_d \sigma_0 \left[R_d - e^{-r/R_d} (r + R_d) \right]. \quad (68)$$

To calculate the mass of dark matter, it is usually assumed that the mass distribution of the dark matter halo per unit volume follows the following profile [31]

$$\rho_{DM}(r) = \frac{\rho_{DM0}}{\left(\frac{r}{r_c}\right)^2 + 1}, \quad (69)$$

where ρ_{DM0} is the density of the dark matter halo at the center of the galaxy and r_c is a critical radius at which the halo density is reduced to half its value at the center. Although most studies interpret this profile as representing the dark matter mass distribution in the galactic halo, there is no clear physical justification for adopting such a profile. By integrating the above equation, the mass of the dark matter halo is obtained as

$$M_{DM} = \int_0^r (4\pi r'^2) \rho_{DM}(r') dr' = 4\pi \rho_{DM0} r_c^2 \left[r - r_c \arctan\left(\frac{r}{r_c}\right) \right]. \quad (70)$$

In the ND model, the rotational velocity relationship is given by the following equation

$$v(r) = \sqrt{\frac{GM_d(r)}{r}}. \quad (71)$$

In the DM model, the mass of the dark matter halo is added to the mass of the galaxy disk in the above equation, and as a result, we will have

$$v(r) = \sqrt{\frac{G[M_d(r) + M_{DM}(r)]}{r}}. \quad (72)$$

In order to examine rotational velocities in the RMOND model, it is necessary to introduce the concept of the transition radius r_t at which the gravitational acceleration is equal

to the transition acceleration a_t . In fact, we consider the transition acceleration a_t as an acceleration at which the gravitational theory has completely changed and entered a very weak gravitational regime in which the RMOND theory effectively holds. It is expected that the transition acceleration a_t is of the order of the reference acceleration a_{ref} or slightly less, because a_{ref} in fact introduces the threshold value of the acceleration at which the gravitational regime changes commence. In fact, the reference acceleration a_{ref} , according to its definition, is equivalent to the Milgrom acceleration a_0 , which is of the order of 10^{-10} m/s^2 . With these considerations, we expect the acceleration a_t to be of the order of the Milgrom acceleration a_0 or slightly less.

In the RMOND model, as in the ND model, it is assumed that the mass of the galaxy only includes the mass of the disk, which is given by Eq. (68). Also, in this model, it is assumed that for distances less than the transition distance r_t , the Newtonian gravitational regime prevails, and as a result, the relationship of the rotational velocity is given by Eq. (71). However, for distances greater than r_t , the gravitational regime changes, and as a result, we use Eq. (65) to calculate the rotational velocity. Therefore, in general, to calculate the rotational velocity in the RMOND model, we use the following equation

$$v(r) = \begin{cases} \sqrt{\frac{G M_d(r)}{r}}, & r \lesssim r_t, \\ \sqrt{\frac{|C_A \epsilon|}{2}} c^{\frac{3\epsilon}{4} + 1} (G \hbar)^{-\frac{\epsilon}{4}} r^{\frac{\epsilon}{2}}, & r \gtrsim r_t. \end{cases} \quad (73)$$

Now we want to constrain the mentioned models using observational data for the galaxy NGC 3198. For this purpose, we develop a computational code that is publicly available². In this code, the multi-chain Monte Carlo (MCMC) method is implemented using the Metropolis-Hastings algorithm. The code is written based on the message passing interface (MPI) method, which executes multiple MCMC chains simultaneously. The chains are periodically synchronized until the Gelman-Rubin diagnostic (\hat{R}) is monitored. In our work, we consider the convergence criterion as $\hat{R} - 1 < 0.01$, which guarantees that the MCMC analysis converges well. For the statistical analysis of MCMC chains, we use the GetDist package [32], which is publicly available³.

The results of our MCMC implementation for the best fit value and constraints with a confidence limit (CL) of 68% for the free and derived parameters in the models under

² <https://github.com/krezzazadeh/MCMC-RMOND>

³ <https://getdist.readthedocs.io/en/latest/>

consideration are given in Table I. In Figs. 1-3, the triangular plots of the one-dimensional and two-dimensional posteriors of the free and derived parameters resulting from the MCMC analysis for the three models under consideration are shown. In the MD model, a degeneracy is observed between the two free parameters ρ_{DM0} and r_c , and therefore, we have fixed the critical radius to the value $r_c = 3.062 \text{ kpc}$. In the case of the RMOND model, we also observed that the MCMC method cannot constrain the free parameters ϵ and r_t properly, and therefore we have fixed these parameters with the values 0.046 and 25.285 kpc, respectively.

TABLE I. The best-fit values and 68% CL constraints for the parameters of the investigated models.

Parameter	ND		DM		RMOND	
	best-fit	68% limits	best-fit	68% limits	best-fit	68% limits
$\tilde{\sigma}_0/10^8$	3.467	3.438 ± 0.034	2.825	2.790 ± 0.058	3.790	3.761 ± 0.040
$R_d [\text{kpc}]$	9.376	9.461 ± 0.090	5.110	6.02 ± 0.36	8.087	8.154 ± 0.083
$\log_{10}(\tilde{\rho}_{\text{DM0}})$	—	—	7.569	$7.502^{+0.035}_{-0.028}$	—	—
$r_c [\text{kpc}]$	—	—	3.062(fixed)	—	—	—
ϵ	—	—	—	—	0.046(fixed)	—
$r_t [\text{kpc}]$	—	—	—	—	25.285(fixed)	—
$M_d [M_\odot]$	1.816×10^{11}	$(1.830 \pm 0.020) \times 10^{11}$	4.626×10^{10}	$(6.33^{+0.64}_{-0.79}) \times 10^{10}$	1.514×10^{11}	$(1.526 \pm 0.017) \times 10^{11}$
$M_{\text{DM}} [M_\odot]$	—	—	1.723×10^{11}	$(1.48 \pm 0.11) \times 10^{11}$	—	—
$M_{\text{tot}} [M_\odot]$	—	—	2.185×10^{11}	$(2.114^{+0.037}_{-0.056}) \times 10^{11}$	—	—
$ C_A $	—	—	—	—	2.835×10^{-8}	$(2.847 \pm 0.023) \times 10^{-8}$
$a_t [m/s^2]$	—	—	—	—	2.782×10^{-11}	$(2.794 \pm 0.023) \times 10^{-11}$

TABLE II. The resulting values of χ^2 for each model and each data set. Here, we have defined $\Delta\chi^2 = \chi^2_{\text{model}} - \chi^2_{\text{DM}}$.

	ND	DM	RMOND
χ^2	277.26	57.12	61.37
$\Delta\chi^2$	220.14	0.0	4.25

We see in Table I that in the ND and RMOND models, the mass of the galaxy disk M_d is of the order $10^{11} M_\odot$, but in the DM model, it is of order $10^{11} M_\odot$ which is one order of magnitude smaller. These predictions can be used to distinguish between these models by considering other methods for measuring the mass of the galactic disk. We further see in the table that in our model, the transition acceleration a_t is obtained of the order

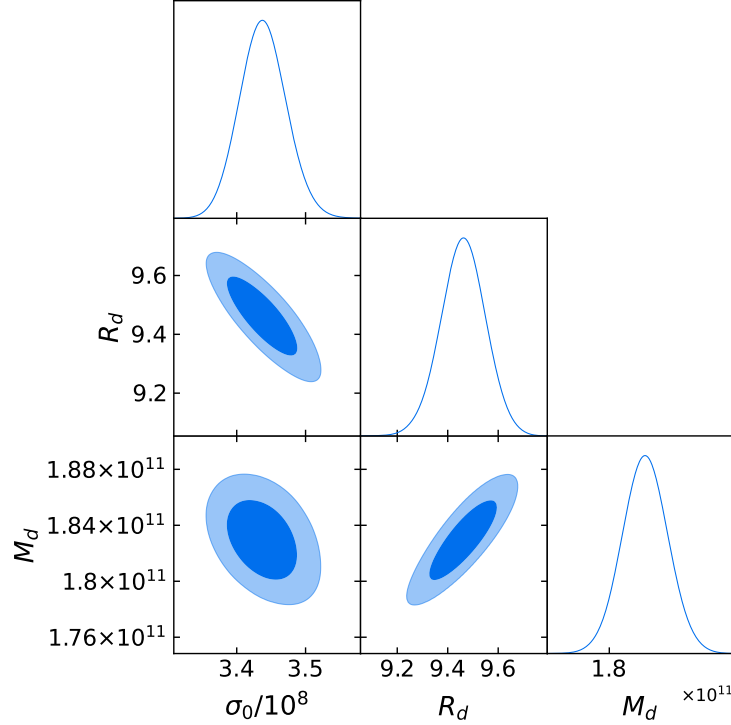


FIG. 1. 1D likelihoods and 2D contours for the parameters in 68% and 95% CL marginalized joint regions for the ND model.

10^{-11} m/s^2 , which is one order of magnitude less than the value for the Milgrom acceleration $a_0 \sim 10^{-10} \text{ m/s}^2$. Of course, here we have calculated a_t at a moment when it is assumed that the new gravitational regime is fully established, so the acceleration at this time is expected to be less than the Milgrom acceleration a_0 that determines the threshold for changing the gravitational regime.

In Table II, the results of the values of the χ^2 quantity in the MCMC implementation for the models under consideration are presented. The following relation gives this quantity as

$$\chi^2 = \sum_i \frac{(v^{(\text{th})}(r_i) - v^{(\text{obs})}(r_i))^2}{\sigma_i^2}, \quad (74)$$

where $v^{(\text{th})}(r_i)$ is equal to the value obtained from the theoretical model under consideration for the rotational velocity at the radial distance r_i , while $v^{(\text{obs})}(r_i)$ denotes the measured value for it. In addition, σ_i represents the error in the measurement of the rotational velocity. The lower the value of χ^2 a theoretical model gives, the better the fit of that model to the observational data. We see in Table II that the value of χ^2 in the DM and RMOND models is much lower than the value obtained in the ND model. Therefore, the two models MD

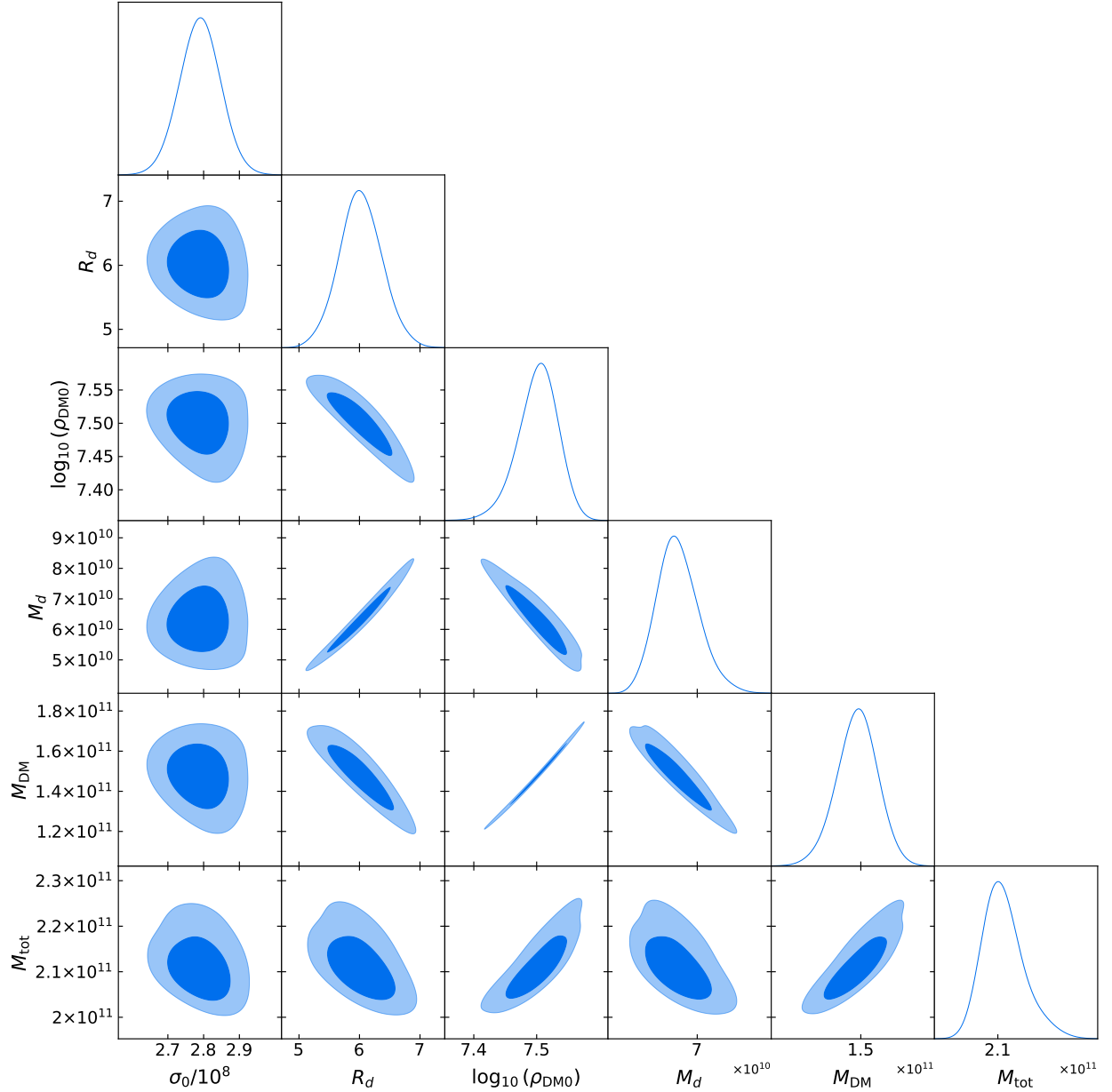


FIG. 2. 1D likelihoods and 2D contours for the parameters in 68% and 95% CL marginalized joint regions for the DM model.

and RMOND, in contrary to the ND model, provide a good fit to the observational data. The DM model gives the lowest value for the χ^2 parameter and, as a result, the best fit is associated with this model. But as we said before, this mass uses a mass profile that has no physical justification. However, our analysis indicates that for large radial distances, namely for $r \gtrsim 20$ kpc, the RMOND scenario provides a considerably better fit to the observational data. To declare this point more clearly, we have plotted the variation of the rotational

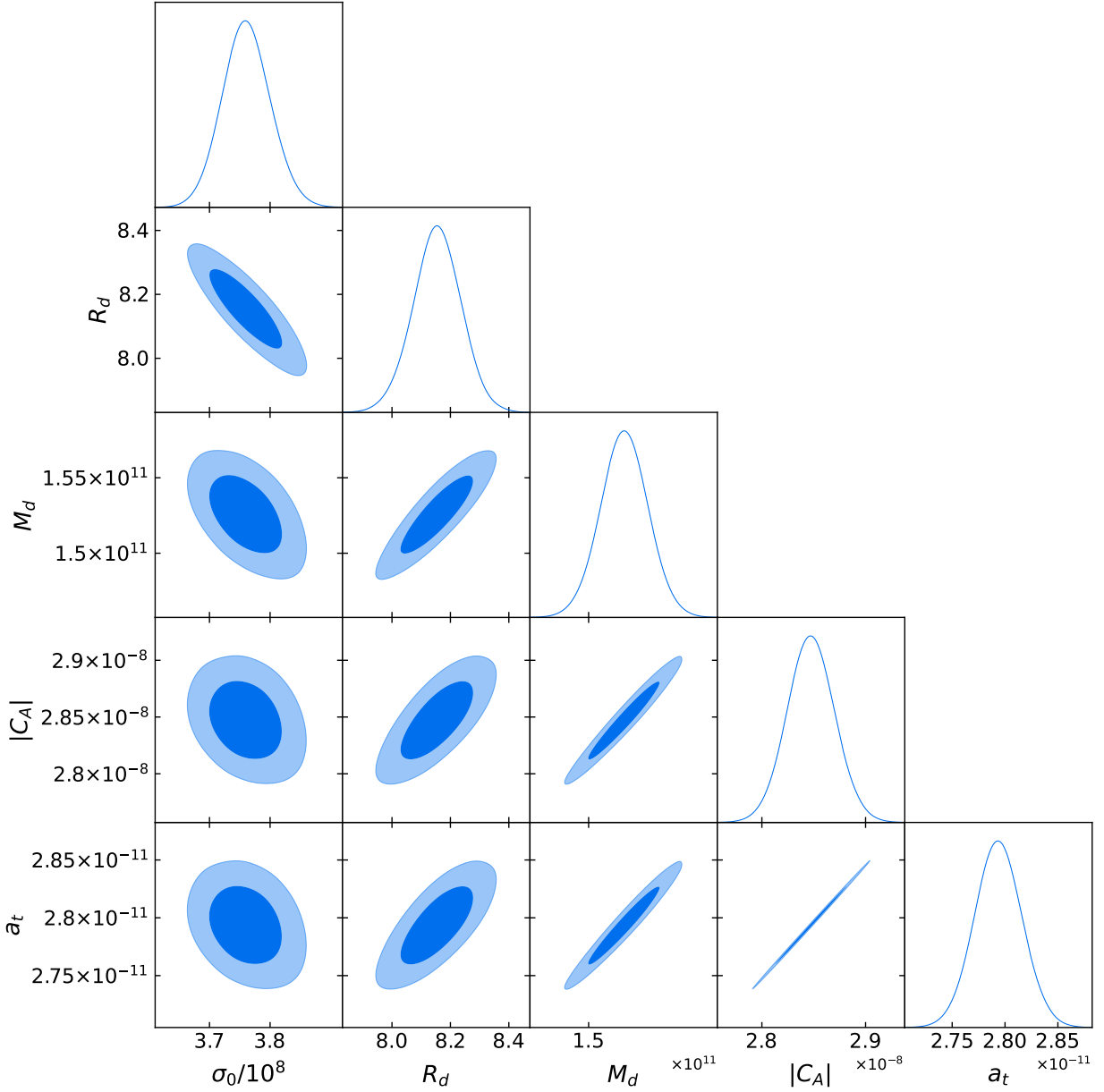


FIG. 3. 1D likelihoods and 2D contours for the parameters in 68% and 95% CL marginalized joint regions for the RMOND model.

velocity with distance in Fig. 4, for the models under consideration. By comparing the plots of the MD and RMOND model in this figure, it is evident that the RMOND model fits the data much more better than the DM model in the radial distances of $r \gtrsim 20$ kpc.

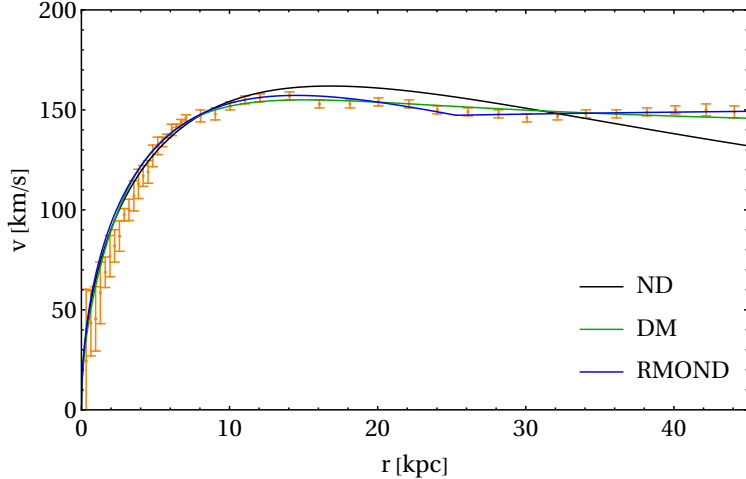


FIG. 4. Rotational velocity versus distance from the galaxy center for the ND, DM, and RMOND models. The data points from the measurements of the galaxy NGC 3198 are also presented in the figure.

V. CONCLUSIONS

In this work, we have explored a relativistic extension of Modified Newtonian Dynamics (MOND) within the framework of entropic gravity. By incorporating temperature-dependent corrections to the equipartition law, one can derive modified Einstein equations that introduce explicit thermal corrections to the geometric sector of gravity. These modifications naturally lead to a characteristic acceleration scale, a_0 , which is consistent with the phenomenology of MOND. This approach provides a theoretical underpinning for MOND, grounded in thermodynamic principles, and extends the framework of entropic gravity proposed by Verlinde and others.

The solutions to the modified Einstein equations for a static, spherically symmetric space-time showed that the metric differs from the standard Schwarzschild solution, yet smoothly reduces to Minkowski space in the low-temperature limit. For accelerations less than a characteristic acceleration, the metric form of the Schwarzschild relation changes to a modified form that determines the geometry of space-time in the very weak gravity limit. This result offers a relativistic foundation for MOND, which has traditionally been a non-relativistic theory.

From an astrophysical perspective, we applied the relativistic MOND (RMOND) model to the galaxy NGC 3198, comparing its predictions with those of classical Newtonian dynamics

(ND) and the dark matter (DM) model. The Bayesian parameter inference showed that the RMOND model provides a better fit to the data at large galactocentric radii ($r \gtrsim 20$ kpc), compared to both the Newtonian and dark matter models. This finding is in line with earlier work, such as [1] and [23], which also explored the validity of MOND in explaining galactic dynamics without invoking dark matter. The RMOND model achieved strong consistency with observational data, providing an alternative explanation to dark matter for galactic rotation curves, especially at large distances where dark matter halos become increasingly difficult to constrain.

Notably, the RMOND model offers a compelling explanation for the observed rotational velocity curves of galaxies, producing a smooth transition from Newtonian dynamics to a MOND-like regime at large radii. This stands in contrast to the dark matter model, which typically requires a halo profile with a specific mass distribution that lacks clear physical justification. The RMOND model, in contrast, requires only the mass of the galaxy disk, offering a simpler, non-dark-matter-based explanation for the observed data.

A. Discussion of Results

The results of our analysis highlight the potential of entropic gravity as a framework for understanding modified gravity at galactic scales. The introduction of temperature-dependent corrections to the equipartition law leads to a modified spacetime geometry that naturally accommodates the acceleration scale a_0 seen in MOND-like deviations from Newtonian gravity. Our analysis also demonstrated that, unlike the standard MOND framework, the RMOND model incorporates relativistic effects, making it more robust for cosmological and large-scale applications.

The comparison with observational data for NGC 3198 showed that RMOND provides an excellent fit to rotation curves, especially at large radii where the dark matter model struggles to capture the true dynamics. In contrast, the purely Newtonian model fails to explain the flatness of rotation curves, a signature feature of MOND. The results suggest that temperature-corrected entropic gravity can successfully reproduce the key features of MOND at galactic scales, while offering a coherent and relativistic framework that avoids the need for dark matter.

B. Future Directions

While the RMOND model provides a promising framework for understanding galactic dynamics, several avenues remain for further investigation:

- **Gravitational Lensing:** One of the most promising directions is to extend the RMOND framework to gravitational lensing. Given that lensing is a direct probe of spacetime geometry, comparing the predictions of RMOND with observed lensing data could provide a critical test of the model. Future observations from the Euclid mission [33] or the *Vera C. Rubin Observatory* [34] could offer significant constraints.
- **Cosmological Evolution:** The implications of RMOND for the large-scale evolution of the universe should be explored. In particular, the role of entropic gravity and thermal corrections in cosmic inflation, the formation of large-scale structures, and the behavior of the cosmic microwave background (CMB) deserves further attention. Investigating the effects of RMOND on cosmological parameters would help assess its broader implications for the standard cosmological model.
- **Galaxy Clusters and Larger Scales:** Applying the RMOND model to galaxy clusters, where the dynamics are more complex, would provide additional tests of its validity at larger scales. This could help clarify whether RMOND can successfully explain the behavior of galaxy clusters, where dark matter models typically dominate.
- **Quantum Gravity:** Another exciting avenue is to explore the connections between entropic gravity and quantum gravity. The emergence of gravity from statistical mechanics, as suggested by the holographic principle and the Unruh effect, could provide new insights into the fundamental nature of gravity at the quantum level. Investigating these connections could lead to a deeper understanding of the potential unification of gravity with quantum mechanics.
- **Multi-Galaxy Datasets:** Finally, a broader observational study using multi-galaxy datasets from upcoming astronomical surveys, such as those planned for the **Vera C. Rubin Observatory**, would provide a more comprehensive test of the model's ability to explain galactic dynamics across different galaxy types, redshifts, and environments.

C. Final Remarks

In summary, this work successfully constructs a relativistic extension of MOND, grounded in entropic gravity, that provides a natural and dark-matter-free explanation for galactic rotation curves. The RMOND model achieves strong agreement with observational data, particularly at large galactic radii, where dark matter models are less constrained. As we continue to refine and extend this framework, the potential for RMOND to reshape our understanding of gravity and cosmology becomes increasingly apparent. With further observational and theoretical work, RMOND may offer a compelling alternative to the dark matter paradigm and provide a deeper understanding of the nature of gravity in our universe.

- [1] M. Milgrom, *Astrophys. J.* **270**, 365 (1983).
- [2] M. Milgrom, *Astrophys. J.* **270**, 371 (1983).
- [3] M. Milgrom, *Astrophys. J.* **270**, 384 (1983).
- [4] R. H. Sanders and S. S. McGaugh, *Ann. Rev. Astron. Astrophys.* **40**, 263 (2002), arXiv:astro-ph/0204521.
- [5] D. Clowe, M. Bradac, A. H. Gonzalez, M. Markevitch, S. W. Randall, C. Jones, and D. Zaritsky, *Astrophys. J. Lett.* **648**, L109 (2006), arXiv:astro-ph/0608407.
- [6] G. W. Angus, B. Famaey, and H. Zhao, *Mon. Not. Roy. Astron. Soc.* **371**, 138 (2006), arXiv:astro-ph/0606216.
- [7] C. Skordis and T. Zlosnik, *Phys. Rev. Lett.* **127**, 161302 (2021), arXiv:2007.00082 [astro-ph.CO].
- [8] J. M. Bardeen, B. Carter, and S. W. Hawking, *Commun. Math. Phys.* **31**, 161 (1973).
- [9] S. W. Hawking, *Nature* **248**, 30 (1974).
- [10] S. W. Hawking, *Commun. Math. Phys.* **43**, 199 (1975), [Erratum: *Commun.Math.Phys.* 46, 206 (1976)].
- [11] J. D. Bekenstein, *Phys. Rev. D* **7**, 2333 (1973).
- [12] W. G. Unruh, *Phys. Rev. D* **14**, 870 (1976).
- [13] T. Jacobson, *Phys. Rev. Lett.* **75**, 1260 (1995), arXiv:gr-qc/9504004.
- [14] E. P. Verlinde, *JHEP* **04**, 029 (2011), arXiv:1001.0785 [hep-th].

- [15] G. 't Hooft, Conf. Proc. C **930308**, 284 (1993), arXiv:gr-qc/9310026.
- [16] L. Susskind, J. Math. Phys. **36**, 6377 (1995), arXiv:hep-th/9409089.
- [17] L. Susskind and J. Lindesay, *An introduction to black holes, information and the string theory revolution: The holographic universe* (2005).
- [18] F. Reif, *Fundamentals of Statistical and Thermal Physics* (McGraw Hill, Tokyo, 1965).
- [19] R. K. Pathria, *Statistical Mechanics*, 2nd ed. (Butterworth-Heinemann, 1996).
- [20] E. P. Verlinde, SciPost Phys. **2**, 016 (2017), arXiv:1611.02269 [hep-th].
- [21] S. Hossenfelder, Phys. Rev. D **95**, 124018 (2017), arXiv:1703.01415 [gr-qc].
- [22] J. D. Bekenstein, Phys. Rev. D **70**, 083509 (2004), [Erratum: Phys.Rev.D 71, 069901 (2005)], arXiv:astro-ph/0403694.
- [23] B. Famaey and S. McGaugh, Living Rev. Rel. **15**, 10 (2012), arXiv:1112.3960 [astro-ph.CO].
- [24] S. S. McGaugh, Phys. Rev. Lett. **106**, 121303 (2011), [Erratum: Phys.Rev.Lett. 107, 229901 (2011)], arXiv:1102.3913 [astro-ph.CO].
- [25] A. Sheykhi and K. Rezazadeh Sarab, JCAP **10**, 012 (2012), arXiv:1206.1030 [physics.gen-ph].
- [26] K. Rezazadeh, (2025), arXiv:2503.08236 [gr-qc].
- [27] R. M. Wald, *General Relativity* (Chicago Univ. Pr., Chicago, USA, 1984).
- [28] E. Poisson, *A relativist's toolkit: the mathematics of black-hole mechanics* (Cambridge university press, 2004).
- [29] S. Weinberg, *Gravitation and cosmology: principles and applications of the general theory of relativity* (John Wiley & Sons, 2013).
- [30] K. C. Freeman, Astrophys. J. **160**, 811 (1970).
- [31] K. G. Begeman, A. H. Broeils, and R. H. Sanders, Mon. Not. Roy. Astron. Soc. **249**, 523 (1991).
- [32] A. Lewis, (2019), arXiv:1910.13970 [astro-ph.IM].
- [33] Y. Mellier *et al.* (Euclid), Astron. Astrophys. **697**, A1 (2025), arXiv:2405.13491 [astro-ph.CO].
- [34] Ž. Ivezić *et al.* (LSST), Astrophys. J. **873**, 111 (2019), arXiv:0805.2366 [astro-ph].